



Functionally Graded Cathodes for Honeycomb Solid Oxide Fuel Cells

Changrong Xia, William Rauch,* William Wellborn, and Meilin Liu**,:z

School of Materials Science and Engineering, Center for Innovative Fuel Cell and Battery Technologies,
Georgia Institute of Technology, Atlanta, Georgia 30332-0245, USA

Functionally graded cathodes were fabricated by slurry coating process for honeycomb solid oxide fuel cells with yttria-stabilized zirconia (YSZ) electrolytes. The cathodes are composed of strontium-doped lanthanum manganate (LSM), gadolinia-doped ceria, and $\text{La}_{0.6}\text{Sr}_{0.4}\text{Co}_{0.2}\text{Fe}_{0.8}\text{O}_3$ (LSCF). The LSM content was gradually decreased, while the LSCF content was gradually increased with the increasing distance away from the electrolyte-electrode interface. Scanning electron microscopy investigation and electrochemical impedance spectroscopy measurements revealed that the electrochemical performance of the graded cathodes depends sensitively on the microstructures that were primarily determined by firing temperatures. The cathodes graded in composition show interfacial resistances about 10 times lower than traditional LSM-YSZ cathodes that have similar microstructures and thickness. The graded cathode fired at low temperature has an interfacial resistance as low as $0.47 \Omega \text{ cm}^2$ at 750°C , which is very encouraging for developing honeycomb fuel cells operated below 800°C .

© 2002 The Electrochemical Society. [DOI: 10.1149/1.1503203] All rights reserved.

Manuscript submitted April 1, 2002; revised manuscript received June 6, 2002. Available electronically August 2, 2002.

In the development of solid oxide fuel cells (SOFCs) both tubular and planar designs are actively pursued around the world. While the tubular design has the advantages of easy manifolding and sealing, its power density is relatively low. The planar design, on the other hand, offers high power density. However, the required manifolding and sealing is more difficult to achieve. Honeycomb fuel cells¹ with alternating layers of electrolyte and metal interconnect, in essence, is an elegant way of miniaturizing and packing tubular cells with high power density but without difficulties in manifolding and sealing. The honeycomb design thus offers the advantages of both tubular and planar design.

In order to achieve the advantages of the honeycomb design it is necessary to develop a novel cathode with high electrochemical performance, which is fabricated utilizing a technique compatible with the honeycomb structures. The development of cathode materials for SOFCs based on yttria-stabilized zirconia (YSZ) has mainly focused on strontium-doped lanthanum manganites (LSM) because this material remains stable in oxidizing atmospheres, has sufficient electrical conductivity at 1000°C , and has a close match in the coefficient of thermal expansion to the YSZ electrolyte. However, single phase LSM does not have acceptable performance due to its low oxygen ion conductivity. One effective approach for improving the performance is to add a secondary phase of higher ionic conductivity to LSM to extend the active area over which the oxygen reduction reaction can occur. YSZ is widely studied as the second phase, and achieves very good performances at high temperatures (800 – 1000°C), but it is not clear if the performance of these cathodes will be sufficient at lower temperatures. To date, their efficient operation at high temperatures imposes considerable restrictions on the materials that can be used in cell construction and in the balance of plant. To overcome these problems, the operating temperature must be lowered, leading to a desire for the development of reduced-temperature ($<800^\circ\text{C}$) SOFCs. The performance of these reduced-temperature SOFCs depends strongly on the cathode/electrolyte interface, since the interfacial resistance (polarization) of the solid-state cells increases rapidly as the operating temperature is decreased.²⁻⁵ At reduced temperatures, it is necessary to add ionic conductors with higher conductivity than YSZ to obtain adequate electrochemical performance. Gadolinia-doped ceria (GDC), which has much higher ionic conductivities than YSZ at reduced temperatures, has been used to replace YSZ to form a GDC-LSM composite electrode. The interfacial polarization resistance of an LSM-GDC

composite cathode is about one-half to one-third that of an LSM-YSZ composite cathode on a YSZ electrolyte when they have similar microstructures.⁶ However, the in-plane electronic conductivity of a composite LSM cathode is relatively low, resulting in large losses due to current collection. The advantages of adding a layer of current collector are demonstrated by the addition of an LSM layer over the LSM/YSZ composite layer.⁷ Strontium-doped lanthanum cobaltite (LSC) has been identified as a cathode material that offers improved electrical conductivity, for example, 1200 S cm^{-1} at 1000°C compared to a typical value of 150 S cm^{-1} for LSM at the same temperature.⁸ Unfortunately LSC has a higher thermal expansion coefficient (TEC, 22 to $24 \times 10^{-6} \text{ K}^{-1}$) than YSZ and LSM (11 – $13 \times 10^{-6} \text{ K}^{-1}$). It has also been shown that LSC readily reacts with YSZ to form a resistive phase.⁸ To avoid sharp discontinuities in TECs, which could result in delamination during thermal cycling, cathodes graded in composition were developed with its electronic conducting phase gradually changed from LSM to LSC.⁹⁻¹¹ Instead of an abrupt change in composition and/or microstructure between the electrochemically active layer and the current collecting layer, functional graded cathodes have a graded interface at which the composition gradually changes from one layer to another.

In this paper, we report our finding on cathodes graded in composition for honeycomb fuel cells fabricated by extrusion. The cathodes, consisting of LSM, $\text{La}_{0.6}\text{Sr}_{0.4}\text{Co}_{0.2}\text{Fe}_{0.8}\text{O}_3$ (LSCF), and GDC with graded composition changes in layers of LSM50 (50 wt % LSM) + GDC50, LSM25 + LSCF25 + GDC50, LSCF50 + GDC50, and LSCF100, were fabricated using a slurry coating process, a technique widely used for applying thin and thick films of porous and dense ceramics to ceramic substrates with planar, tubular, and other complex shaped structures. The observed electrochemical performances of the graded cathodes were impressive for developing honeycomb YSZ fuel cells operated at temperatures below 800°C .

Submicrometer powders of GDC ($\text{Gd}_{0.1}\text{Ce}_{0.9}\text{O}_{1.95}$), LSM ($\text{La}_{0.85}\text{Sr}_{0.15}$)_{0.9}MnO₃, and LSCF ($\text{La}_{0.6}\text{Sr}_{0.4}\text{Co}_{0.2}\text{Fe}_{0.8}\text{O}_3$) were prepared using a glycine-nitrate process with stoichiometric amount of nitrates (Aldrich).^{12,13} The glycine to nitrate mole ratio was set at 0.5. The powders were preheated at 600 , 850 , and 1150°C for 4 h, respectively, to form the fluorite (GDC) and perovskite (LSM, LSCF) structures, as determined by X-ray diffraction analysis. The oxide powders were made into slurries by ballmilling the oxides for 24 h with proper amount of organic binder, and acetone. Symmetric cells were fabricated by coating all channels of YSZ honeycomb with cathode slurries; the oxide weight ratios were set at LSM:GDC = 50:50, LSM:LSCF:GDC = 25:25:50, LSCF:GDC

* Electrochemical Society Student Member.

** Electrochemical Society Active Member.

z E-mail: meilin.liu@mse.gatech.edu

Table I. Compositions of the cathode samples prepared. (Their interfacial polarization resistances are presented in Fig. 3.)

Sample no.	Layer 1	Layer 2	Layer 3	Layer 4	Firing
1	LSM50-YSZ50	LSM50-YSZ50	LSM50-YSZ50	LSM50-YSZ50	1100°C
2	LSM50-GDC50	LSM50-GDC50	LSM50-GDC50	LSM50-GDC50	1100°C
3	LSM50-GDC50	LSM50-GDC50	LSCF50-GDC50	LSCF50-GDC50	1100°C
4	LSM50-GDC50	LSM50-GDC50	LSCF50-GDC50	LSCF100	1100°C
5	LSM50-GDC50	LSM25-LSCF25-GDC50	LSCF50-GDC50	LSCF100	1050-1200°C

= 50:50, and pure LSCF. The slurries were subsequently coated onto the inner channels of the YSZ honeycombs, that were fabricated by extrusion of YSZ (8% mol Y_2O_3) powder, and followed by sintering in air at 1350°C for 12 h. The fired honeycomb has 16 channels (4×4) with wall thicknesses of 300 μm , and a distance between adjacent walls of 1.6 mm. It was cut into short pieces; about 30 mm long. The coated layer was dried at 120°C for 2 h, and fired at 1050-1100°C for 2 h before a successive layer was applied. The multilayers were finally fired at 1050~1200°C for 4 h with a heating and cooling rate of 5 and 10°C per min, respectively. LSM-YSZ cathodes for honeycomb YSZ were also prepared for comparison by slurry coating under the same processing conditions as that used for the LSM-GDC cathodes. Table I lists the compositions and firing temperatures of the samples tested in this study.

Electrochemical impedance measurements were carried out using a Solartron 1255 HF frequency response analyzer in combination with a Solartron 1286 electrochemical interface. Measurements were taken without a dc bias, and spectra were obtained in a frequency range typically from 1 MHz to 10 mHz with an applied ac voltage amplitude of 60 mV. All the samples were measured in air at temperatures increasing from 550 to 800°C in 50°C intervals. Silver wires were attached to the electrodes with a silver paste, and a thermocouple was positioned close to the sample to provide an accurate measurement of the sample temperature. All data were taken 30 minutes after the desired temperature was reached. The data was corrected for electrode area ($0.16 \times 3.0 \text{ cm}^2$), and divided by two (symmetric cell) to obtain the actual interfacial polarization resistance of each electrolyte/electrode interface.

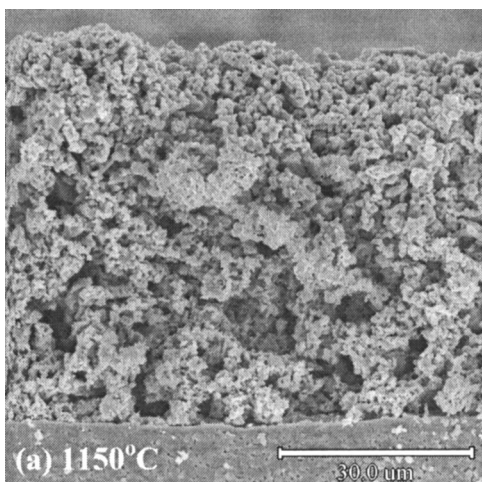
Figure 1a shows a scanning electron microscope (SEM) image of a graded LSM-LSCF-GDC cathode (sample 5) fired at 1150°C for 4 h. A homogeneous distribution of particles and pores is seen over the distance from the solid electrolyte interface to the top of the cathode. No distinguishable variation in microstructures is observed across the four individual layers. However, the thickness of each individual layer was revealed by SEM investigations of the sample after each successive slurry coating procedure. Thicknesses for the total cathode after each coating and firing at 1100°C are: LSM50-GDC50: 12-14 μm , LSM25-LSCF25-GDC50: 25-30 μm , LSCF50-GDC50: 38-45 μm , and LSCF: 50-60 μm . The thickness of the entire compositionally graded cathode is approximately 56 μm , as shown in Fig. 1a.

The SEM examination revealed that the microstructures of all the samples fired at the same temperature were very similar. However, the firing temperature has a strong influence on the microstructures. Figure 1b and c illustrate the microstructures of the LSM50-GDC50 layer that were developed by firing at 1050 and 1200°C, respectively. Figure 1b indicates neck formation between adjacent particles. A higher magnification image showed that smaller particles had coarsened and formed larger aggregates. There was a high level of interconnected porosity, and the LSM50-GDC50 layer appeared to have good adhesion with the YSZ honeycomb. At the higher (Fig. 1c) temperature it is seen that the aggregates formed from the smaller particles were much larger: the size was approximately 1-2 μm compared to 0.1-0.3 μm when fired at 1050°C. Figure 1c also shows excellent bonding between the LSM50-GDC50 cathode and YSZ honeycomb.

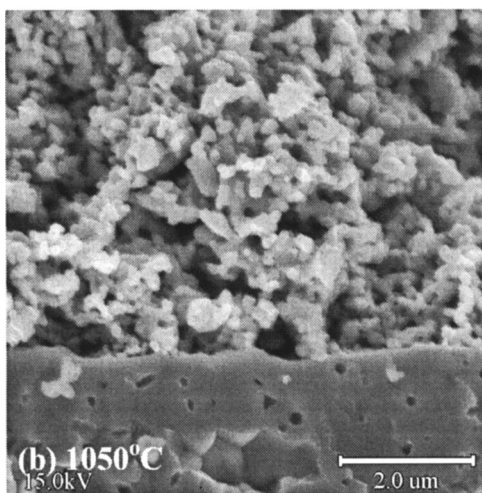
Shown in Fig. 2 is a typical impedance spectrum measured at

750°C for a honeycomb cell with a four-layer GDC-LSM-LSCF cathode (sample 5) sintered at 1100°C with its layer composition changed from LSM50-GDC50, to LSM25-LSCF25-GDC50, to LSCF50-GDC50, and to LSCF. An ohmic resistance, R_e (intercept between the impedance arc at high frequencies and the real axis), and an interfacial polarization impedance (difference between high frequency and low frequency intercept with the real axis) can be distinguished. As the measurement temperature decreased, the total impedance represented by the curve increased. In the two-electrode configuration, the observed interfacial polarization impedance corresponds to the sum of all resistances arising from the electrochemical processes in both electrodes, which is twice that of the single electrode polarization resistance and denoted by $2Rp$. In an ideal symmetrical cell, as in the honeycomb structure, the contribution of each electrode is half of the total impedance. Thus half of the measured $2Rp$ is used to evaluate the cathode performance. The ohmic resistance in the test circuit, R_e , the difference between the origin and the high frequency intercept of the impedance with the real axis, is determined by residual losses in the test circuit including the ionic resistance of the electrolyte layer, the electronic resistance of the cathodes, and the electrical contact resistance between the cell and the measurement system.

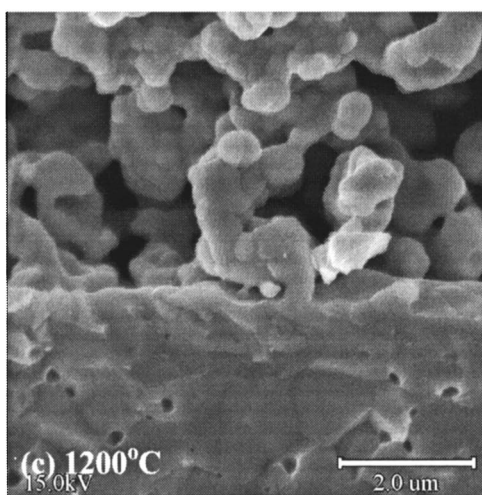
It is observed that, at a given temperature, the interfacial polarization resistances of GDC-LSM cathodes (sample 2, 1.5 $\Omega \text{ cm}^2$ at 800°C) are about one-half to one-fourth those of YSZ-LSM cathodes (sample 1, 5.1 $\Omega \text{ cm}^2$ at 800°C). Comparing to YSZ, using GDC as the oxygen ion conducting phase in the composite cathodes dramatically increased the cathode performance of LSM since GDC is more conductive than YSZ. GDC-LSM is therefore used as the electrochemically active layer in the cathodes for honeycomb fuel cells. It is found that the interfacial polarization of sample 5 at 800°C (0.46 $\Omega \text{ cm}^2$) is less than one-tenth that of sample 1 (5.1 $\Omega \text{ cm}^2$). Shown in Fig. 3 is the temperature dependence of interfacial resistances for cathodes that were fabricated using similar procedures, which have similar microstructures such as porosity, thickness, and grain size as revealed with SEM. The cathode with gradually changed composition (sample 5) shows the best electrochemical performance, whereas the cathode consisting of four identical layers of LSM50-GDC50 (sample 2) displayed the highest interfacial resistance since the electrical conduction in the LSM50-GDC50 layers is relative low, which will result in inefficient electron supply to the triple phase boundaries (TPB), where the electron reacts with oxygen ion vacancies and oxygen to form oxygen ions. Eventually cathodic performance is improved as shown in Fig. 3 by replacing LSM with LSCF, which is known to be much more conductive than LSM. For example, at 750°C interfacial resistance decreased from 2.6 $\Omega \text{ cm}^2$ (sample 2), to 1.5 $\Omega \text{ cm}^2$ (sample 3), and 1.1 $\Omega \text{ cm}^2$ (sample 4), and further decreased to 0.90 $\Omega \text{ cm}^2$ (sample 5) for the cathode with the smoothest change of composition between two neighboring layers. Because the mismatch of the TEC of LSCF with those of LSM, GDC, and YSZ, undesired microcracks may be introduced by mechanical stresses under thermal cycling during electrode fabrication and SOFC operation. Some severe microcracks may electrically disconnect parts of the geometric area within the cathode or at the interface to the solid electrolyte. Those isolated domains may range from micrometer scale to large



(a)



(b)



(c)

Figure 1. Scanning electron micrographs (SEMs) of the cross section of graded cathodes fired at (a) 1150°C, (b) 1050°C, and (c) 1200°C.

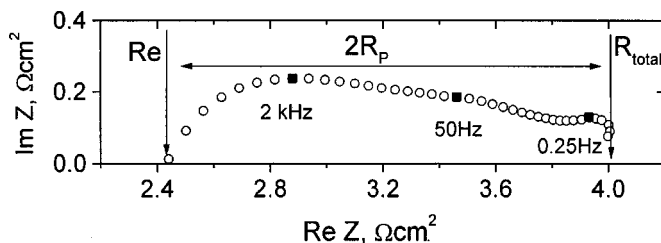


Figure 2. An impedance spectrum measured at 750°C for a compositionally graded cathode (sample 5) fired at 1100°C for 4 h.

dimensions leading to high interfacial resistances, since only those TPB areas electrically connected to the top of the porous collecting layer can be used during operation of the electrode. The gradual change in composition of sample 5 minimizes the thermal mismatch, and eventually suppresses microcracks, leading to improved electrical contact throughout the electrode. Much better performance is therefore expected through finer incremental changes in composition; for example, changing the composition in 10% intervals.

Shown in Fig. 4 is the reciprocal temperature dependence of interfacial resistance of graded cathodes (sample 5) fired at 1050–1200°C. The activation energy for the resistance is also shown in Fig. 4. The benefits of using a lower firing temperature are clearly illustrated here. The interfacial resistance at 750°C is 3.1 Ω cm² for a cathode fired at 1200°C, and decreases to 0.47 Ω cm² for that at 1050°C. Meanwhile the activation energy decreases from 1.45 eV for the cathode fired at 1200°C to 1.12 eV for that fired at 1050°C. The decrease in cathodic performance at high firing temperature is in accordance with a decreased length of the TPB in a coarse structure due to the large average particle size developed during high temperature firing. Figure 1b and c clearly show that high temperature firing cause some physical changes in the cathodes, such as a reduction in porosity, and a decrease in contact area between the ionic and electronic components.

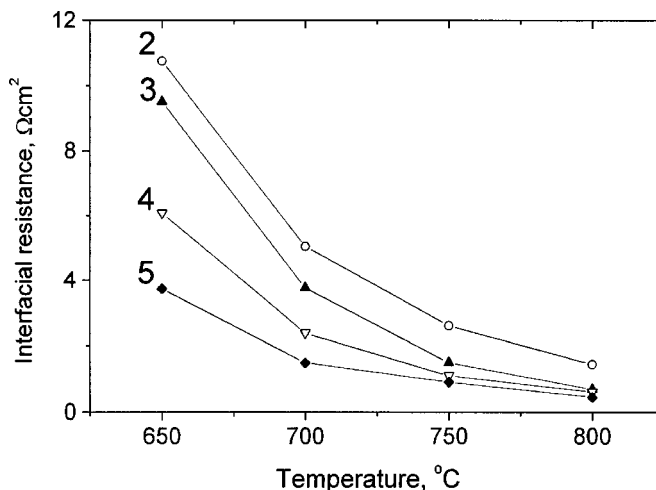


Figure 3. Interfacial polarization resistances measured at different temperatures for cathodes with different composition. The number adjacent to each curve represents the sample number as listed in Table I.

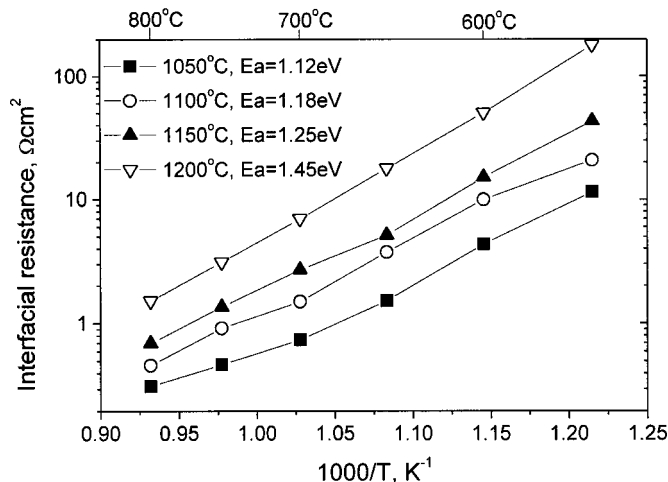


Figure 4. Arrhenius plot of the polarization resistance of compositionally graded cathodes (sample 5) fired at 1050-1200°C for 4 h.

Acknowledgment

The authors wish to gratefully acknowledge Kevin Hurysz, J. K. Lee, and Joe Cochran for fabrication of the YSZ honeycomb samples. The authors also wish to gratefully acknowledge the support of this research by National Science Foundation (grant no.

CTS-9819850), DoE-NETL (grant no. DE-FG26-01NT41274), and the DARPA/DSO Palm Power program directed by Robert Nowak and funded through ARMY/ARO grant no. DAAD19-01-1-0649 monitored by Richard Paur.

The Georgia Institute of Technology assisted in meeting the publication costs of this article.

References

1. C. R. Xia, W. Rauch, J. Cochran, J. Lee, and M. L. Liu, in *Proceedings of the 1st International Conference on Materials Processing for Properties and Performance (MP3)*, Nanyang Technology University and Institute of Materials (East Asia), Aug 1, 2002.
2. B. C. H. Steele, K. M. Hori, and S. Uchino, *Solid State Ionics*, **135**, 445 (2000).
3. R. Doshi, Von L. Richards, J. D. Carter, X. Wang, and M. Krumpelt, *J. Electrochem. Soc.*, **146**, 1273 (1999).
4. C. R. Xia, F. L. Chen, and M. L. Liu, *Electrochem. Solid-State Lett.*, **4**, A52 (2001).
5. C. R. Xia and M. L. Liu, *Adv. Mater.*, **14**, 521 (2002).
6. E. P. Murray, and S. A. Barnett, *Solid State Ionics*, **143**, 265 (2001).
7. M. J. Jorgenson, S. Primdahl, C. Bagger, and M. Mogensen, *Solid State Ionics*, **139**, 1 (2001).
8. N. Q. Minh and T. Takahashi, *Science and Technology of Ceramic Fuel Cells*, Elsevier Science, Amsterdam (1995).
9. N. T. Hart, N. P. Brandon, M. J. Day, and J. E. Shemilt, *J. Mater. Sci.*, **36**, 1077 (2001).
10. N. T. Hart, N. P. Brandon, M. J. Day, and N. Lapena-Rey, *J. Power Sources*, **106**, 42 (2002).
11. P. Holtappels and C. Bagger, *J. Eur. Ceram. Soc.*, **22**, 41 (2002).
12. C. R. Xia and M. L. Liu, *Solid State Ionics*, **144**, 249 (2001).
13. C. R. Xia and M. L. Liu, *J. Am. Ceram. Soc.*, **84**, 1903 (2001).